DOI: 10.1002/ejic.201100662

Azide-Bridged Copper(II) and Manganese(II) Compounds with a Zwitterionic Tetrazolate Ligand: Structures and Magnetic Properties

Xiu-Bing Li,[a] Yu Ma,[a] Xiu-Mei Zhang,[a] Jian-Yong Zhang,[a] and En-Qing Gao*[a]

Keywords: Coordination polymers / Copper / Magnetic properties / Manganese / Azides

Two azide-bridged coordination polymers, $[Cu(mptz)(N_3)_2]$ (**1**) and $[Mn(mptz)(N_3)_2H_2O]$ (**2**), (mptz = *N*-methyl-4-pyridinium tetrazolate), were synthesized and crystallographically and magnetically characterized. Compound **1** is a neutral 1D coordination polymer in which the Cu^{II} ions, which are in a square pyramidal surrounding, are linked by double end-on azide bridges in an alternating basal–basal and basal–apical fashion. Compound **2** exhibits a 3D Mn^{II}–azide coordination framework with the (10,3)-*b* net topology, in which the double end-on–azide-bridged dimanganese units are interlinked by single end-to-end azide bridges. The magnetic analyses indicated that **1** behaves magnetically as a quasi-dimer with an $S = 1$ ground state due to a strong ferromagnetic interaction through the basal–basal azide bridges and a very weak antiferromagnetic coupling through the basal–apical azide bridges. Compound **2** exhibits 3D antiferromagnetic behaviors with $T_N = 24.0$ K, where the end-to-end and end-on azide bridges mediate the antiferromagnetic and ferromagnetic interactions, respectively.

Introduction

The field of molecular magnetism has attracted much attention and seen great progress in recent years. It has focused on revealing the magneto-structural correlations in molecular systems, understanding the underlying physics, and constructing new magnetic materials with potential technological applications.[1–3] Many material with various topologies or intriguing magnetic properties, in which the paramagnetic metal ions are held in close proximity by the short bridging ligands, have been synthesized.[4–5] The connection of the paramagnetic centers by short pseudo-halide ligands is an important strategy that has been used to access these materials. Particular interest has focused on the azide ligand because of its efficiency in ferromagnetic (FM) or antiferromagnetic (AF) coupling, as well as its diversity in its coordination modes μ-1,1 (end-on, EO), μ-1,3 (end-to-end, EE), μ-1,1,3 and so forth, and polymeric bridging networks. In addition, a large number of azide-bridged complexes with different dimensionalities and various topologies have been reported in the literature,[5–7] which include many long-range ordering materials and a few single-molecule/-chain magnets (SMMs and SCMs).[5,6,8] Particular attention has focused on magnetic systems that have a three-dimensional (3D) coordination network.[9–13] However, 3D metal–azide networks are still rare in comparison to the large number of 1D and 2D systems. Among the known examples, some are reinforced by embedded organic bridges,[9–11] while others contain no additional bridges but have embedded non-bridging organic ligands[12] or have hosted cationic guests (Cs^+ or Me_4N^+).[13] The metal ions that are contained in the 3D metal–azide networks are mainly Cu^{II}[12c–12e] and Mn^{II},[11,12a,12b,13] and in a few cases, Co^{II}[9a–9c] and Fe^{II}.[9d]

Recently, we have demonstrated that the zwitterionic carboxylate ligands can lead to 1D, 2D, or 3D systems with mixed azide and carboxylate bridges, which show diverse magnetic properties such as ferromagnetic coupling,[14a,14b] solvent-modulated metamagnetism,[14c,14d] and SCMs.[14d–14f] As an extension of this study, we turned to the zwitterionic tetrazolate ligands, which remain largely unexplored in coordination chemistry, although the tetrazolate ligands are evoking increasing interest.[15] In this paper we report on two coordination compounds that have a zwitterionic tetrazolate ligand, *N*-methyl-4-pyridinium tetrazolate (mptz). The compounds are formulated as $[Cu(mptz)(N_3)_2]$ (**1**) and $[Mn(mptz)(N_3)_2H_2O]$ (**2**). Compound **1** is composed of chains that have alternating basal–basal and basal–apical EO–azide bridges, while compound **2** exhibits a novel 3D Mn^{II}–azide coordination framework

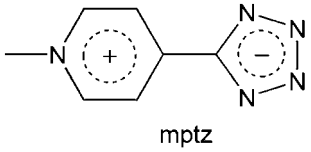

mptz

Scheme 1. The chemical structure of mptz.

[a] Shanghai Key Laboratory of Green Chemistry and Chemical Processes, Department of Chemistry, East China Normal University,
Shanghai 200062, China
Fax: +86-21-62233404
E-mail: eqgao@chem.ecnu.edu.cn

Supporting information for this article is available on the WWW under http://dx.doi.org/10.1002/ejic.201100662.

with mixed EE and EO bridges. The mptz ligand in both of the compounds adopts the terminal coordination mode. The magnetic analyses indicated that **1** exhibits alternating FM and AF interactions along the chain while **2** exhibits long-range AF ordering (Scheme 1).

Results and Discussion

Description of the Structures

The Structure of 1

The Cu^{II} coordination environment of compound **1** is depicted in Figure 1 (a) and the selected bond lengths and angles are listed in Table 1. The asymmetric unit contains one Cu^{II} atom, one mptz ligand, and two azide ions. The unique Cu^{II} ion assumes an elongated square pyramidal geometry where the basal plane is formed by three azide nitrogen atoms (N8, N8A, and N9) and a tetrazolate nitrogen atom (N3) and the apical position is occupied by another azide nitrogen atom (N9B). The basal Cu–N distances are in the narrow range of 1.9620(15) to 2.0110(15) Å while the apical distance is significantly longer [2.6626(19) Å]. A least-squares plane calculation showed that the CuN_4 base unit is essentially planar with a maximum deviation of 0.0883(19) Å from the mean plane. The structure of **1** can be viewed as being made up of dinuclear neutral units with the formula $[Cu_2(mptz)_2(N_3)_4]$, which results from the assembly of two Cu^{II} spheres through two equivalent symmetric EO–azide bridges with a Cu···Cu bond length of 3.1537(3) Å. The azide bridges are arranged between the Cu^{II} ions in the basal–basal fashion, that is, the bridging nitrogen atoms lie in the basal planes of both of the Cu^{II} ions. The bridging angle of Cu1–N8–Cu1A is 103.32(7)° and the $[Cu_2N_2]$ four-membered ring is planar. The neighboring dinuclear units are connected through the double asymmetric EO–azide bridges, which are disposed in the basal–apical fashion with long (apical) and short (basal) Cu–N distances. Therefore, a 1D-chain that has alternating basal–basal and basal–apical azide bridges was formed and is shown in Figure 1 (b). The Cu···Cu distance and the Cu–N–Cu angle for the basal–apical azide bridge is 3.3927(3) Å and 92.969(61)°, respectively. All of the chains in the structure are parallel to the *a* direction and there are plenty of interchain weak C–H···N hydrogen bonds (see Supporting Information, Figure S1). The nearest interchain Cu···Cu distance is 9.4435(4) Å.

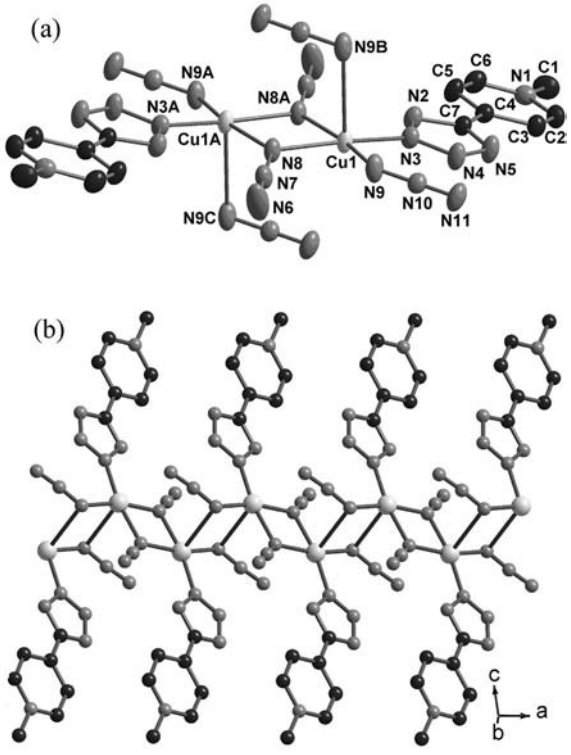

Figure 1. (a) The coordination environment of the Cu^{II} ions in **1** with the atom labeling scheme. The thermal ellipsoids are drawn at the 50% probability level (A, 2 – *x*, –*y*, 2 – *z*; B, 1 – *x*, –*y*, 2 – *z*; C, 1 + *x*, *y*, *z*). (b) The 1D azide-bridged Cu^{II} chain.

Table 1. Selected bond lengths [Å] and angles [°] for compounds **1** and **2**.[a]

1			
Cu1–N3	1.9620(15)	Cu1–N9	1.9698(17)
Cu1–N8A	2.0090(16)	Cu1–N8	2.0110(15)
N3–Cu1–N9	97.80(7)	N3–Cu1–N8A	96.05(7)
N9–Cu1–N8A	166.07(7)	N3–Cu1–N8	169.94(7)
N9–Cu1–N8	89.76(7)	N8A–Cu1–N8	76.68(7)
N6–N7–N8	178.1(2)	N7–N8–Cu1A	133.30(13)
N7–N8–Cu1	121.69(13)	Cu1A–N8–Cu1	103.32(7)
N10–N9–Cu1	134.28(14)	N11–N10–N9	175.0(2)
2			
Mn1–N1	2.1737(19)	Mn1–N6	2.1775(17)
Mn1–O1	2.1939(15)	Mn1–N5	2.2318(16)
Mn1–N5A	2.2765(17)	Mn1–N10	2.3064(16)
N1–N2	1.1618(19)	N3–N4	1.158(3)
N4–N5	1.175(2)	N6–N7	1.1617(17)
N9–N10	1.324(2)	N10-N11	1.316(2)
N11-N12	1.339(2)	N1–Mn1–N6	92.86(8)
N1–Mn1–O1	88.71(7)	N6–Mn1–O1	89.49(7)
N1–Mn1–N5	96.80(7)	N6–Mn1–N5	170.24(7)
O1–Mn1–N5	89.36(6)	N1–Mn1–N5A	171.59(7)
N6–Mn1–5A	91.94(7)	O1–Mn1–N5A	84.43(6)
N5–Mn1–5A	78.30(6)	N1–Mn1–N10	94.59(7)
N6–Mn1–N10	87.02(6)	O1–Mn1–N10	175.31(6)
N5–Mn1–N10	93.56(6)	N5A–Mn1–N10	92.56(6)
N1–N2–N1B	176.1(3)	N3–N4–N5	177.9(2)
N6–N7–N6C	180.0	N11–N10–N9	109.95(15)
N10-N11–12	108.86(16)	N9–N10–Mn1	116.07(12)

[a] For compound **1**, A: 2 – *x*, –*y*, 2 – *z*; for compound **2**, A: –*x*, 1 – *y*, 1 – *z*; B: –*x*, *y*, 1/2 – *z*; C: 1/2 – *x*, 1/2 – *y*, 1 – *z*.

The Structure of 2

Compound **2** exhibits a 3D Mn^{II}–azide network with the (10,3)-*b* topology. The atom numbering scheme is depicted in Figure 2 (a) and the relevant bond parameters are collected in Table 1. The asymmetric unit consists of one Mn^{II} ion, one mptz ligand, two azide ions, and one aqua molecule. Each Mn^{II} center is octahedrally coordinated by four equatorial azide nitrogen atoms (N1, N5, N6, and N5A), a tetrazolate nitrogen atom, and an aqua oxygen atom, with

the Mn–N/O distances ranging from 2.1737(19) to 2.3064(16) Å. Two neighboring Mn^{II} ions, which are related by an inversion center, are doubly linked by two EO–azide bridges (N5 and N5A) to form a binuclear unit. In the Mn_2N_2 planar ring that results, the Mn–N–Mn bridging angle is 101.70(6)° and the Mn···Mn distance is 3.4962(5) Å. The EO–azide groups deviate somewhat from the Mn_2N_2 ring [N5A–N5–N4 170.63(15)°]. Each dimeric $[Mn(\mu\text{-EO-}N_3)_2Mn]^{2+}$ fragment is linked to four identical motifs by means of four single EE–azide bridges, which generates a neutral 3D Mn^{II}–azide lattice (Figure 2, c). The structure features three different chain motifs with alternating azide bridges (Figure 2, b). There are two independent sets of EE–azide bridges. One of the EE–azide sets, where the central nitrogen atom (N2) is on the crystallographic C_2 axes, links the dimeric units into chains with alternating EO and EE bridges along the *c* direction. The Mn–N···N–Mn torsion angle and the Mn···Mn distance for the EE bridge is 84.955(275)° and 6.2047(12) Å, respectively. The other EE–azide set lies at the inversion centers, where the Mn–N···N–Mn torsion angle is 180° and the Mn···Mn distance is 6.281(1) Å, and links the dimeric units into equivalent chains along the [110] and [1–10] directions, which also have alternating EO and EE bridges. The third chain motif is along the [101] direction and is formed by the alternation of the different EE bridges. The 3D Mn^{II}–azide lattice results from the sharing of the metal ions by the three independent chain sets (Figure 2, c). The "voids" in the lattice are occupied by the terminally coordinated mptz ligands, with O–H···N hydrogen bonds between the coordinated water molecules and the tetrazole groups (see Supporting Information, Figure S2).

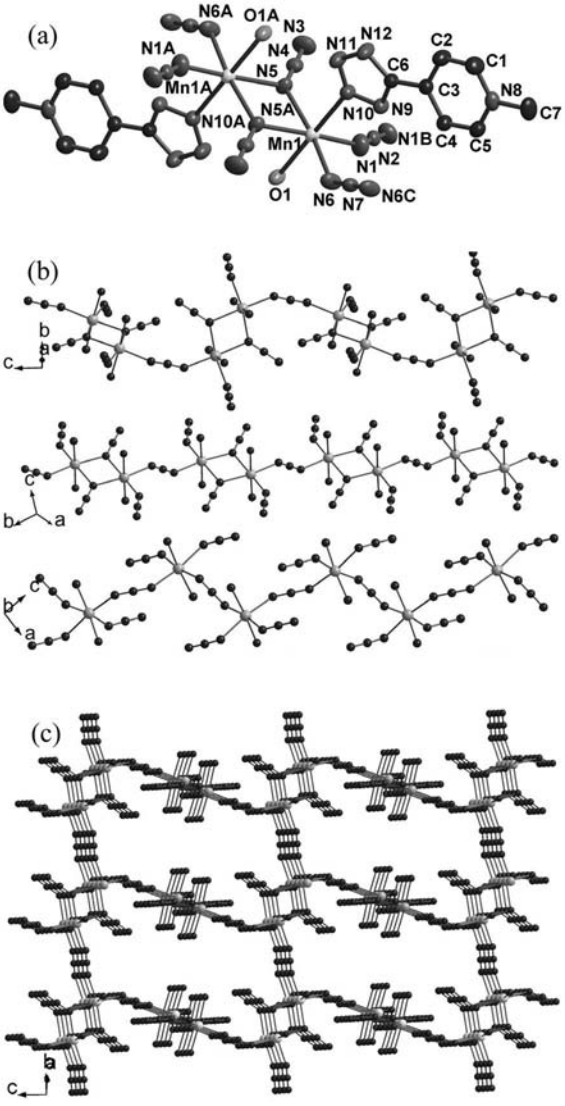

Figure 2. (a) The dicuclear unit in **2** with the atom labeling scheme. The thermal ellipsoids are drawn at the 50% probability level (A, $-x$, $1-y$, $1-z$; B, $-x$, y, $1/2-z$; C, $1/2-x$, $1/2-y$, $1-z$). (b) Three independent chain motifs with the alternating azide bridges in **2**. (c) The 3D network for **2**.

The complicated 3D network could be better illustrated with the help of topological analysis. By simplifying the double EO and single EE–azide bridges into linear linkers between the nodes (Mn ions), the 3D network is reduced to a 3-connected net with the (10,3)-*b* topology [point symbol: 10^3, which is denoted **ths** according to the Reticular Chemistry Structure Resource (RCSR) nomenclature][16] (Figure 3). Alternatively, by taking the EO–azide-bridged dimers as nodes, the network becomes 4-connected with a $CdSO_4$-type topology (point symbol: $6^5.8$, which is denoted as **cds**; see also Supporting Information, Figure S3).

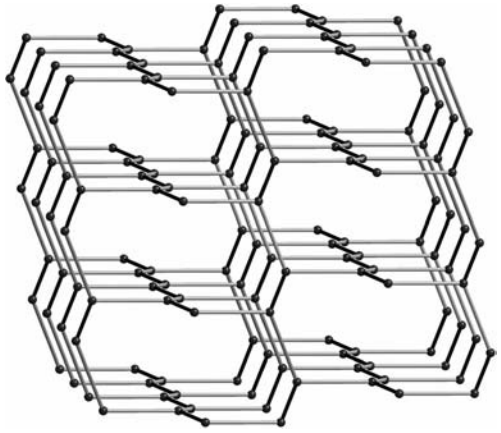

Figure 3. The sketch map of the (10,3)-*b* net in **2** (black rods for double EO–azide connections, and grey ones for single EE connections).

It is interesting to note that the 3D Mn^{II}–azide network is in contrast with the 2D networks in which each dimeric $[Mn(\mu\text{-EO-}N_3)_2Mn]^{2+}$ fragment is also connected to four identical motifs by single EE–azide bridges. These Mn^{II}–azide layers, which have the 2D honeycomb 6^3 topology, have been reported in many systems.[17] Two different 3D Mn^{II}–azide networks that are based on such motifs have been reported in the previous papers. In one of them, each dimeric fragment is connected to six neighbors by EE–azide ligands, which results in a 5-connected 3D net with the hexagonal BN topology ($4^6{\cdot}6^4$, **bnn**).[13a] In the other one, the

dimeric units are connected by means of single EE–azide bridges and also by methylpyrazine bridges to give another 5-connected $4^6{\cdot}6^4$ net (**zga**)[11e] according to our topological analysis.[16a] It is interesting to note that the net topology is the same as that found in **2** if the methylpyrazine is omitted.

Magnetic Properties

The magnetic susceptibility (χ) of compound **1** was measured in the range of 2 to 300 K and is shown as the χT and χ versus T plots in Figure 4. The measured χT value at 300 K is approximately 0.96 emu mol^{-1} K per dimer, which is higher than the spin-only value (0.75 emu mol^{-1} K with g = 2.00) for two magnetically isolated S = 1/2 ions. Upon cooling, the χ value increases monotonically but the χT value increases up to a maximum value of 1.18 emu mol^{-1} K at 10 K and then drops slightly. The data above 100 K follows the Curie–Weiss law with C = 0.90 emu mol^{-1} K and θ = 14.80 K. The high-temperature behavior suggests that the FM interactions dominate in this compound, and the maximum χT value is close to that expected for an S = 1 state.

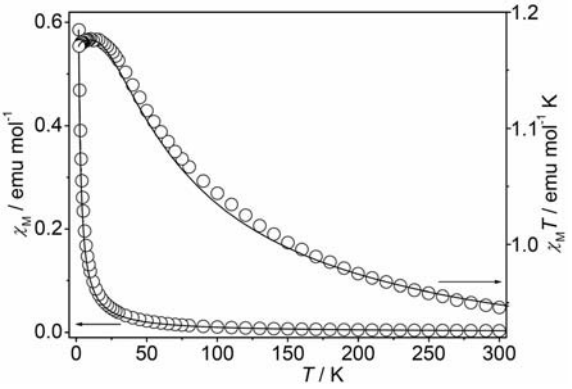

Figure 4. The temperature-dependence of χ and χT for **1** under 1 kOe. The solid lines represent the best fit to the Bleaney–Bowers equation.

According to the structural data, there are two alternating sets of double EO–azide bridges between the Cu^{II} ions in **1** (Figure 1, b). One set is in the basal–basal fashion and the other set is in the basal–apical fashion. Two J parameters are needed in order to account for the magnetic interactions in the chain. This system may be simplified by considering the magneto-structural features. Because the magnetic orbital of Cu^{II} in the axially elongated square pyramidal field is of the $d_{x^2-y^2}$ type and is mainly delocalized over the basal ligands, the magnetic exchange is principally propagated through the basal–basal bridge, and the exchange through the basal–apical bridge should be much weaker.[18] This is especially true for the systems where Cu^{II} shows little or no deviation from the equatorial plane, as was observed in **1**. Thus, the alternating chain in **1** can be treated as a quasi-dimeric system, which has strong intradimeric magnetic interactions (J) through the basal–basal bridges and much weaker interdimeric interactions (J') through the basal–apical bridges. The magnetic behaviors could be analyzed by the Bleaney–Bowers equation – see Equation (1)[19] – in combination with the molecular-field approximation, see Equation (2), z = 2.[1a]

$$\chi_{dimer} = (2Ng^2\beta^2)/kT/[3 + \exp(-J/kT)] \quad (1)$$

$$\chi = \chi_{dimer}/[1 - (zJ'\chi_{dimer}/Ng^2\beta^2)] \quad (2)$$

Here, the Hamiltonian for the dimeric unit is $H = -JS_1{\cdot}S_2$. The best fit over the whole temperature range led to J = 65.4 cm^{-1}, g = 2.17, and J' = –0.0055 cm^{-1}. The positive J value confirms a strong intradimeric FM interaction through the double basal–basal EO–azide bridges, while the small negative J' value suggests a weak interdimeric AF coupling through the basal–apical EO–azide bridges. It has been suggested that the FM interaction through the double basal–basal EO–azide bridges generally decreases as the Cu–N–Cu angle or the Cu–N length increases. Theoretical calculations have indicated a crossover from FM to AF interactions at approximately 104°.[20a] A collection of the magnetic and structural data for the previous Cu^{II} dimeric compounds have been given elsewhere.[20b] Compound **1** lies in the FM regime and follows the general trend. The interaction is weaker than those for the compounds with similar Cu–N distances and smaller Cu–N–Cu angles.[20b,21] The interaction in **1** is similar in magnitude to those for two previous Cu^{II} dimmers,[22] which have smaller Cu–N–Cu angles, longer Cu–N distances, and a larger distortion in the square pyramidal geometry. For the asymmetric basal–apical EO–azide bridges, negligible to weak interactions, FM or AF, have been reported and no magneto-structural correlations have been deduced.[23]

The dominating FM interaction in **1** was confirmed by the isothermal magnetization at 2 K (Figure 5). As the field is lifted, the magnetization approaches saturation more rapidly than was predicted from the Brillouin function for two isolated Cu^{II} ions (the dashed line in Figure 5). The

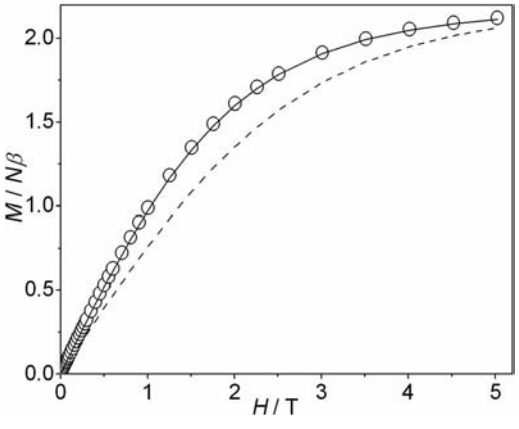

Figure 5. The field-dependent isothermal magnetization curve for compound **1** at 2 K. The solid and dash lines represent the Brillouin curves that were calculated for S = 1 and for the two uncoupled S = 1/2 spins, respectively, with g = 2.18.

experimental curve was well fitted by the Brillouin function for $S = 1$, with $g = 2.18$. This clearly supports the quasi-dimeric character of the system in term of the magnetism.

The temperature-dependence of the magnetic susceptibility (χ) for compound **2** at an applied field of 1 kOe is shown in Figure 6. The χT value per Mn^{II} at 300 K is approximately 4.1 emu mol^{-1} K, which is close to the spin-only value (4.38 emu mol^{-1} K) that is expected for a magnetically isolated high-spin Mn^{II} ion with $g = 2.00$. As the temperature is lowed, the χT value decreases continuously, whereas the χ value first increases to a maximum of 0.049 emu mol^{-1} K at 35 K and then decreases rapidly to 0.037 emu mol^{-1} K at 2 K. The observations that the χ value extrapolated to 0 K is about two-thirds of the χ_{max} value and that the $d(\chi T)/dT$ curve shows a λ-type anomaly at 24.0 K indicate that **2** behaves as a 3D antiferromagnet with $T_N = 24.0$ K.[24] The data above 100 K follows the Curie–Weiss law with $C = 4.6$ emu mol^{-1} K and $\theta = -33.1$ K. The ratio for $T_N/|\theta|$ of 0.73 conforms well to the range for the 3D Heisenberg AF character.[25]

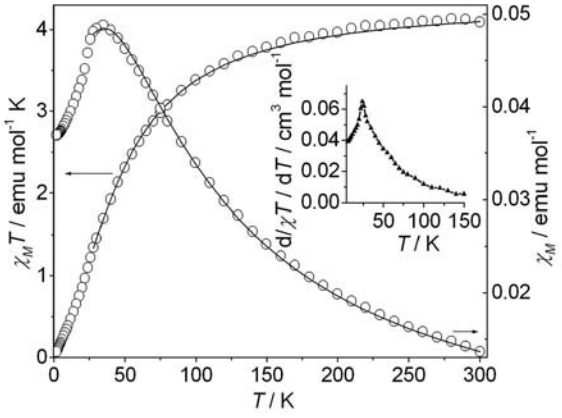

Figure 6. The temperature-dependence of χ and χT for **2**. The solid lines represent the fit to the model for the uniform chains (see the text). Inset: The differential of χT.

The 3D AF character suggests that the AF interactions are predominant in the compounds but does not preclude the existence of FM interactions. It has been demonstrated by many Mn^{II} compounds that the interaction between the azide-bridged Mn^{II} ions is FM for the EO mode, where the Mn–N–Mn bond angle in the usual range of 99 to 105°, but that the interaction is always AF for the EE bridging mode.[26] It is worth noting that theoretical calculations predicted AF interactions for the EO–azide where the Mn–N–Mn bond angle is less than 98°, which has recently been experimentally illustrated by a tetranuclear system.[27] For **2**, the Mn–N–Mn bond angle is 101.70(6)°. Therefore, we assumed that compound **2** exhibits FM and AF interactions through the double EO and single EE–azide bridges, respectively. In order to evaluate the magnetic interactions, we applied an approximate approach that has been used for similar 2D layers.[17b] This approach treats the network as EE–azide-bridged AF chains that interact ferromagnetically through the double EO–azide bridges. The AF interaction (J) through the EE–azide bridge can be accounted for by the conventional equation derived by Fisher for a uniform chain of classical spins based on the Hamiltonian $H = -JS_i \cdot S_{i+1}$ equation, see Equation (3).[28]

$$\chi_{chain} = [Ng^2\beta^2S(S + 1)/(3kT)][(1 + u)/(1 - u)] \quad (3)$$

where $u = \coth[JS(S + 1)/kT] - kT/[JS(S + 1)]$ and $S = {}^5/_2$.

The interaction through the EO–azide bridges is included by the assumption of an interchain interaction (J') in the molecular field approximation [Equation (2), replacing χ_{dimer} for χ_{chain}, $z = 4$]. The least-squares fit of the experimental data above 28 K led to $J = -5.91$ cm^{-1} and $J' = 0.99$ cm^{-1} with g fixed at 2.00. The above values are in agreement with the general observation for the Mn^{II} ions that the AF interaction through the single EE bridges is stronger in magnitude than the FM interaction through the double EO bridge.[17]

Conclusions

We have presented the syntheses, structures, and magnetic properties of two azide-bridged Cu^{II} and Mn^{II} coordination polymers that were derived from a zwitterionic pyridinium-tetrazolate ligand. In compound **1** the square pyramidal Cu^{II} ions are linked to form chains by double end-on azide bridges in an alternating basal–basal and basal–apical fashion. In compound **2** the dimeric $[Mn(\mu\text{-EO-}N_3)_2\text{-}Mn]^{2+}$ fragments are linked by means of single EE–azide bridges to form a 3D Mn^{II}–azide framework with the (10,3)-*b* net topology. The zwitterionic ligand in both of the compounds adopts the terminal coordination mode through the tetrazolate group. The magnetic investigations revealed that compound **1** has strong intradimeric magnetic interactions through the basal–basal EO–azide bridges and much weaker interdimeric interactions through the basal–apical EO–azide bridges. Compound **2** exhibits FM and AF interactions through the double EO and single EE–azide bridges, respectively, and behaves as a 3D antiferromagnet with $T_N = 24$ K.

Experimental Section

Materials and physical measurements: All of the solvents and reagents for the synthesis were commercially available and were used as received. The ligand mptz was synthesized according to the literature methods.[29] The infrared spectra were recorded with a NEXUS 670 FTIR spectrometer by using the KBr pellets. The elemental analysis was carried out with an Elementar Vario El III elemental analyzer. The temperature and field-dependent magnetic measurements were carried out with a Quantum Design SQUID MPMS-5 magnetometer. The diamagnetic corrections were made with Pascal's constants.

$[Cu(mptz)(N_3)_2]$ (1): A mixture of $CuCl_2 \cdot 2H_2O$ (0.10 mmol, 17 mg), mptz (0.10 mmol, 16 mg), NaN_3 (0.20 mmol, 13 mg), and H_2O (8 mL) was sealed in a Teflon-lined autoclave and heated to 100 °C. After 5 days, the reaction vessel was cooled to room temperature over 12 h and the pure black block crystals were collected (approxi-

mately 64% based on $CuCl_2 \cdot 2H_2O$). $C_7H_7CuN_{11}$ (308.78): calcd. C 27.23, H 2.29, N 49.90; found C 26.95, H 2.46, N 49.65. IR (KBr): $\tilde{\nu}$ = 3054 (m), 2089 (s), 2045 (s), 1641 (s), 1572 (m), 1545 (m), 1472 (m), 1348 (s), 1309 (m), 1191 (m), 1133 (m), 1012 (m), 867 (m), 530 (m) cm^{-1}.

$[Mn(mptz)(N_3)_2H_2O]$ (2): A mixture of $MnCl_2 \cdot 4H_2O$ (0.10 mmol, 20 mg), mptz (0.10 mmol, 16 mg), and NaN_3 (0.20 mmol, 13 mg) in CH_3OH (10 mL) was stirred for 30 min at 60 °C. A clear brown solution was obtained and was subsequently cooled to room temperature over several days to give compound **2** as transparent yellow crystals (approximately 48%). $C_7H_9MnN_{11}O$ (318.19): calcd C 26.43, H 2.85, N 48.43; found C 26.87, H 2.51, N 48.01. IR (KBr): $\tilde{\nu}$ = 3248 (m), 2094 (s), 1637 (s), 1540 (m), 1468 (m), 1332 (m), 1278 (s), 1218 (m), 1179 (m), 1128 (m), 860 (m), 680 (m) cm^{-1}.

Crystal Data Collection and Refinement: The diffraction intensity data were collected at 293 K with a Bruker APEX II diffractometer that was equipped with a CCD area detector and graphite-monochromated Mo-K_α radiation (λ = 0.71073 Å). The empirical absorption corrections were applied by using the SADABS program.[30] The structures were solved by the direct method and were refined by the full-matrix least-squares method on F^2, with all of the non-hydrogen atoms refined with anisotropic thermal parameters.[31] The hydrogen atoms that were attached to the carbon atoms were placed in calculated positions and were refined by using the riding model, and the hydrogen atoms of the water molecules in compound **2** were located from the difference maps. The pertinent crystallographic data and structure refinement parameters are summarized in Table 2.

Table 2. The crystal data and structure refinements for compounds **1** and **2**.

	1	**2**
Formula	$C_7H_7CuN_{11}$	$C_7H_9MnN_{11}O$
M_r	308.78	318.19
Temperature [K]	296	296
Crystal system	monoclinic	monoclinic
Space group	$P2_1/n$	$C2/c$
a [Å]	5.2971(2)	12.898(3)
b [Å]	16.2625(5)	12.382(2)
c [Å]	13.1013(4)	15.593(3)
α [°]	90	90
β [°]	98.2440(10)	92.623(2)
γ [°]	90	90
V [Å^3]	1116.94(6)	2487.7(8)
Z	4	8
D_c [g cm^{-3}]	1.836	1.699
μ [mm^{-1}]	1.963	1.079
Reflections collected	14815	5017
Unique reflections/R_{int}	2742/0.0219	2202/0.0216
R_1 [$I > 2\sigma(I)$]	0.0259	0.0301
wR_2(All data)	0.0747	0.0876
GOF	1.034	1.071

CCDC-831671 (for **1**) and -831672 (for **2**) contain the supplementary crystallographic data for this paper. These data can be obtained free of charge from The Cambridge Crystallographic Data Centre via www.ccdc.cam.ac.uk/data_request/cif.

Supporting Information (see footnote on the first page of this article): Diagrams showing the 3D packing structures in **1** and **2** and the 3D net topology of **2**.

Acknowledgments

We are thankful for the financial support from the National Natural Science Foundation of China (NSFC) (grant number 91022017) and the Fundamental Research Funds for the Central Universities.

[1] a) O. Kahn, *Molecular Magnetism*, Wiley-VCH, Weinheim, Germany, **1993**; b) D. Gatteschi, O. Kahn, J. S. Miller, F. Palacio, *Magnetic Molecular Materials*, Kluwer Academic, Dordrecht, The Netherlands, **1991**; c) C. Coulon, H. Miyasaka, R. Clérac, *Struct. Bonding (Berlin)* **2006**, *122*, 163–206.

[2] a) J. S. Miller, A. J. Epstein, *Angew. Chem.* **1994**, *106*, 399; *Angew. Chem. Int. Ed. Engl.* **1994**, *33*, 385–415; b) E. Coronado, P. Delhaes, D. Gatteschi, J. S. Miller (Eds.), *Molecular Magnetism: from Molecular Assemblies to the Devices*, NATO ASI Series 15, Kluwer, Dordrecht, The Netherlands, **1995**, vol. 321.

[3] a) J. S. Miller, *Adv. Mater.* **2002**, *14*, 1105–1110; b) J. S. Miller, M. Drillon (Eds.), *Magnetism: Molecules to Materials*, Wiley-VCH, Weinheim, Germany, **2002–2005**, vols. I–V; c) D. Gatteschi, R. Sessoli, *Angew. Chem.* **2003**, *115*, 278; *Angew. Chem. Int. Ed.* **2003**, *42*, 268–279.

[4] a) M. Ohba, H. Okawa, *Coord. Chem. Rev.* **2000**, *198*, 313–328; b) S. R. Batten, K. S. Murray, *Coord. Chem. Rev.* **2003**, *246*, 103–130; c) R. Lescouëzec, L. M. Toma, J. Vaissermann, M. Verdaguer, F. S. Delgado, C. Ruiz-Pérez, F. Lloret, M. Julve, *Coord. Chem. Rev.* **2005**, *249*, 2691–2729; d) E. Coronado, P. Day, *Chem. Rev.* **2004**, *104*, 5419–5448; e) D. R. Talham, *Chem. Rev.* **2004**, *104*, 5479–5502.

[5] a) J. Ribas, A. Escuer, M. Monfort, R. Vicente, R. Cortés, L. Lezama, T. Rojo, *Coord. Chem. Rev.* **1999**, *193*, 1027–1068; b) A. Escuer, G. Aromí, *Eur. J. Inorg. Chem.* **2006**, 4721–4736; c) X.-Y. Wang, Z.-M. Wang, S. Gao, *Chem. Commun.* **2008**, 281–294; d) Y.-F. Zeng, X. Hu, F.-C. Liu, X.-H. Bu, *Chem. Soc. Rev.* **2009**, *38*, 469–480.

[6] a) T. C. Stamatatos, K. A. Abboud, W. Wernsdorfer, G. Christou, *Angew. Chem.* **2007**, *119*, 902; *Angew. Chem. Int. Ed.* **2007**, *46*, 884–888; b) Y.-Z. Zhang, W. Wernsdorfer, F. Pan, Z.-M. Wang, S. Gao, *Chem. Commun.* **2006**, 3302–3304; c) C. I. Yang, W. Wernsdorfer, G. H. Lee, H. L. Tsai, *J. Am. Chem. Soc.* **2007**, *129*, 456–457; d) T. C. Stamatatos, K. A. Abboud, W. Wernsdorfer, G. Christou, *Angew. Chem.* **2008**, *120*, 6796; *Angew. Chem. Int. Ed.* **2008**, *47*, 6694–6698.

[7] a) Z.-F. Ju, Q.-X. Yao, W. Wu, J. Zhang, *Dalton Trans.* **2008**, 355–362; b) B. Bitschnau, A. Egger, A. Escuer, F. A. Mautner, B. Sodin, R. Vicente, *Inorg. Chem.* **2006**, *45*, 868–876; c) A. Escuer, R. Vicente, M. A. S. Goher, F. A. Mautner, *J. Chem. Soc., Dalton Trans.* **1997**, 4431–4434; d) G. Lazari, T. C. Stamatatos, C. P. Raptopoulou, V. Psycharis, M. Pissas, S. P. Perlepes, A. K. Boudalis, *Dalton Trans.* **2009**, 3215–3221; e) K. C. Mondal, P. S. Mukherjee, *Inorg. Chem.* **2008**, *47*, 4215–4225.

[8] a) D.-F. Weng, Z.-M. Wang, S. Gao, *Chem. Soc. Rev.* **2011**, *40*, 3157–3181; b) Z.-X. Li, Y.-F. Zeng, H. Ma, X.-H. Bu, *Chem. Commun.* **2010**, *46*, 8540–8542; c) T.-F. Liu, D. Fu, S. Gao, Y.-Z. Zhang, H.-L. Sun, G. Su, Y.-J. Liu, *J. Am. Chem. Soc.* **2003**, *125*, 13976–13977; d) H.-L. Sun, Z.-M. Wang, S. Gao, *Chem. Eur. J.* **2009**, *15*, 1757–1764; e) J. H. Yoon, D. W. Ryu, H. C. Kim, S. W. Yoon, B. J. Suh, C. S. Hong, *Chem. Eur. J.* **2009**, *15*, 3661–3665.

[9] a) S.-L. Liang, Z.-L. Liu, C.-M. Liu, X.-W. Di, J. Zhang, D.-Q. Zhang, *Z. Anorg. Allg. Chem.* **2009**, *635*, 549–553; b) F. A. Mautner, L. Ohrström, B. Sodin, R. Vicente, *Inorg. Chem.* **2009**, *48*, 6280–6286; c) E.-Q. Gao, P.-P. Liu, Y.-Q. Wang, Q. Yue, Q.-L. Wang, *Chem. Eur. J.* **2009**, *15*, 1217–1226; d) A.-H. Fu, X.-Y. Huang, J. Li, T. Yuen, C.-L. Lin, *Chem. Eur. J.* **2002**, *8*, 2239–2247.

[10] a) L. Cheng, W.-X. Zhang, B.-H. Ye, J.-B. Lin, X.-M. Chen, *Eur. J. Inorg. Chem.* **2007**, 2668–2676; b) H.-J. Chen, Z.-W. Mao, S. Gao, X.-M. Chen, *Chem. Commun.* **2001**, 2320–2321; c) E.-Q. Gao, Z.-M. Wang, C.-H. Yan, *Chem. Commun.* **2003**,

1748–1749; d) E.-Q. Gao, A.-L. Cheng, Y.-X. Xu, M.-Y. He, C.-H. Yan, *Inorg. Chem.* **2005**, *44*, 8822–8835; e) Y. Ma, X.-B. Li, X.-C. Yi, Q.-X. Jia, E.-Q. Gao, C.-M. Liu, *Inorg. Chem.* **2010**, *49*, 8092–8098.

[11] a) C.-M. Liu, Z. Yu, R.-G. Xiong, K. Liu, X.-Z. You, *Inorg. Chem. Commun.* **1999**, *2*, 31–34; b) H.-Y. Shen, D.-Z. Liao, Z.-H. Jiang, S.-P. Yan, B.-W. Sun, G.-L. Wang, X.-K. Yao, H.-G. Wang, *Chem. Lett.* **1998**, 469–470; c) A. Escuer, R. Vicente, F. A. Mautner, M. A. S. Goherc, M. A. M. Abu-Youssef, *Chem. Commun.* **2002**, 64–65; d) Q. Yang, J.-P. Zhao, B.-W. Hu, X.-F. Zhang, X.-H. Bu, *Inorg. Chem.* **2010**, *49*, 3746–3751; e) R. Vicente, B. Bitschnau, A. Egger, B. Sodin, F. A. Mautner, *Dalton Trans.* **2009**, 5120–5126.

[12] a) M. A. S. Goher, F. A. Mautner, *Croat. Chem. Acta* **1990**, *63*, 559–564; b) A. Escuer, R. Vicente, M. A. S. Goher, F. A. Mautner, *Inorg. Chem.* **1996**, *35*, 6386–6391; c) K. C. Mondal, P. S. Mukherjee, *Inorg. Chem.* **2008**, *47*, 4215–4225; d) Z.-G. Gu, Y.-F. Xu, X.-J. Yin, X.-H. Zhou, J.-L. Zuo, X.-Z. You, *Dalton Trans.* **2008**, 5593–5602; e) Z.-G. Gu, J.-L. Zuo, X.-Z. You, *Dalton Trans.* **2007**, 4067–4072.

[13] a) M. A. S. Goher, J. Cano, Y. Journaux, M. A. M. Abu-Youssef, F. A. Mautner, A. Escuer, R. Vicente, *Chem. Eur. J.* **2000**, *6*, 778–784; b) F. A. Mautner, R. Cortes, L. Lezama, T. Rojo, *Angew. Chem.* **1996**, *108*, 96; *Angew. Chem. Int. Ed. Engl.* **1996**, *35*, 78–80; c) F. A. Mautner, S. Hanna, R. Cortes, L. Lezama, M. G. Barandika, T. Rojo, *Inorg. Chem.* **1999**, *38*, 4647–4652.

[14] a) Y. Ma, J.-Y. Zhang, A.-L. Cheng, Q. Sun, E.-Q. Gao, C.-M. Liu, *Inorg. Chem.* **2009**, *48*, 6142–6151; b) Y. Ma, Y.-Q. Wen, J.-Y. Zhang, E.-Q. Gao, C.-M. Liu, *Dalton Trans.* **2010**, *39*, 1846–1854; c) W.-W. Sun, C.-Y. Tian, X.-H. Jing, Y.-Q. Wang, E.-Q. Gao, *Chem. Commun.* **2009**, 4741–4743; d) Y.-Q. Wang, W.-W. Sun, Z.-D. Wang, Q.-X. Jia, E.-Q. Gao, Y. Song, *Chem. Commun.* **2011**, 6386–6388; e) Q.-X. Jia, H. Tian, J.-Y. Zhang, E.-Q. Gao, *Chem. Eur. J.* **2011**, *17*, 1040–1051; f) X.-M. Zhang, Y.-Q. Wang, K. Wang, E.-Q. Gao, C.-M. Liu, *Chem. Commun.* **2011**, 1815–1817.

[15] a) H. Zhao, Z.-R. Qu, H.-Y. Ye, R.-G. Xiong, *Chem. Soc. Rev.* **2008**, *37*, 84–100; b) X. He, C.-Z. Lu, D.-Q. Yuan, *Inorg. Chem.* **2006**, *45*, 5760–5766; c) M. Dinca, A. F. Yu, J. R. Long, *J. Am. Chem. Soc.* **2006**, *128*, 8904–8913; d) W. Ouellette, A. V. Prosvirin, K. Whitenack, K. R. Dunbar, J. Zubieta, *Angew. Chem.* **2009**, *121*, 2174; *Angew. Chem. Int. Ed.* **2009**, *48*, 2140–2143; e) G. Aromí, L. A. Barrios, O. Roubeau, P. Gamez, *Coord. Chem. Rev.* **2011**, *255*, 485–546.

[16] a) V. A. Blatov, A. P. Shevchenko, TOPOS 4.0, Samara State University, Russia, see also http://www.topos.ssu.samara.ru/; b) O'Keeffe, M.; Peskov, M. A.; Ramsden, S. J.; Yaghi, O. M. *Acc. Chem. Res.* **2008**, 41, 1782–1789, see also Reticular Chemistry Structure Resource (RCSR), http://rcsr.anu.edu.au/.

[17] a) A. Escuer, F. A. Mautner, M. A. S. Goher, M. A. M. Abu-Youssef, R. Vicente, *Chem. Commun.* **2005**, 605–607; b) E.-Q. Gao, Y.-F. Yue, S.-Q. Bai, Z. He, S.-W. Zhang, C.-H. Yan, *Chem. Mater.* **2004**, *16*, 1590–1596; c) Z. Shen, J.-L. Zuo, Z. Yu, Y. Zhang, J.-F. Bai, C.-M. Che, H.-K. Fun, J. J. Vittal, X.-Z. You, *J. Chem. Soc., Dalton Trans.* **1999**, 3393–3398; d) A. Escuer, J. Cano, M. A. S. Goher, Y. Journaux, F. Lloret, F. A. Mautner, R. Vicente, *Inorg. Chem.* **2000**, *39*, 4688–4695; e) A. Escuer, R. Vicente, M. A. S. Goher, F. A. Mautner, *Inorg. Chem.* **1997**, *36*, 3440–3446; f) S.-Q. Bai, E.-Q. Gao, Z. He, C.-J. Fang, Y.-F. Yue, C.-H. Yan, *Eur. J. Inorg. Chem.* **2006**, 407–415; g) E.-Q. Gao, S.-Q. Bai, Z.-M. Wang, C.-H. Yan, *J. Am. Chem. Soc.* **2003**, *125*, 4984–4985; h) E.-Q. Gao, Y.-F. Yue, S.-Q. Bai, Z. He, C.-H. Yan, *J. Am. Chem. Soc.* **2004**, *126*, 1419–1429.

[18] a) P.-P. Liu, A.-L. Cheng, N. Liu, W.-W. Sun, E.-Q. Gao, *Chem. Mater.* **2007**, *19*, 2724–2726; b) S. Triki, J. C. Gómez-García, E. Ruiz, J. Sala-Pala, *Inorg. Chem.* **2005**, *44*, 5501–5508; c) S.-Q. Bai, E.-Q. Gao, Z. He, C.-J. Fang, C.-H. Yan, *New J. Chem.* **2005**, *29*, 935–941.

[19] B. Bleaney, K. D. Bowers, *Proc. R. Soc. London, Ser. A* **1952**, *214*, 451–459.

[20] a) E. Ruiz, J. Cano, S. Alvarez, P. Alemany, *J. Am. Chem. Soc.* **1998**, *120*, 11122–11129; b) W.-W. Sun, X.-B. Qian, C.-Y. Tian, E.-Q. Gao, *Inorg. Chim. Acta* **2009**, *362*, 2744–2748.

[21] a) A. Escuer, M. A. S. Goher, F. A. Mautner, R. Vicente, *Inorg. Chem.* **2000**, *39*, 2107–2112; b) J. Comarmond, P. Plumeré, J.-M. Lehn, Y. Agnus, R. Louis, R. Weiss, O. Kahn, I. Morgenstern-Badarau, *J. Am. Chem. Soc.* **1982**, *104*, 6330–6340.

[22] S. Youngme, T. Chotkhun, S. Leelasubcharoen, N. Chaichit, C. Pakawatchai, G. A. van Albada, J. Reedijk, *Polyhedron* **2007**, *26*, 725–735.

[23] S.-Q. Bai, E.-Q. Gao, Z. He, C.-J. Fang, C.-H. Yan, *New J. Chem.* **2005**, *29*, 935–941.

[24] a) M. E. Fisher, *Proc. R. Soc. London A* **1960**, *254*, 66–85; b) M. E. Fisher, *Philos. Mag.* **1962**, *7*, 1731–1734; c) R. L. Carlin, *Magnetochemistry*, Springer-Verlag, Berlin, **1986**.

[25] G. C. DeFotis, E. D. Remy, C. W. Scherrer, *Phys. Rev. B* **1990**, *41*, 9074–9086.

[26] a) R. Cortés, J. L. Pizarro, L. Lezama, M. I. Arriortua, T. Rojo, *Inorg. Chem.* **1994**, *33*, 2697–2700; b) M. Villanueva, J. L. Mesa, M. K. Urtiaga, R. Cortés, L. Lezama, M. I. Arriortua, T. Rojo, *Eur. J. Inorg. Chem.* **2001**, 1581–1586; c) M.-M. Yu, Z.-H. Ni, C.-C. Zhao, A.-L. Cui, H.-Z. Kou, *Eur. J. Inorg. Chem.* **2007**, 5670–5676; d) E.-Q. Gao, S.-Q. Bai, Y.-F. Yue, Z.-M. Wang, C.-H. Yan, *Inorg. Chem.* **2003**, *42*, 3642–3649.

[27] Y. Ma, K. Wang, E.-Q. Gao, Y. Song, *Dalton Trans.* **2010**, *39*, 7714–7722.

[28] M. E. Fisher, *Am. J. Phys.* **1964**, *32*, 343–348.

[29] W. Holzer, C. Jäger, *Monatsh. Chem.* **1992**, *123*, 1027–1036.

[30] G. M. Sheldrick, *Program for Empirical Absorption Correction of Area Detector Data*, University of Göttingen, Germany, **1996**.

[31] G. M. Sheldrick, *SHELXTL*, version 5.1., Bruker Analytical X-ray Instruments Inc., Madison, Wisconsin, **1998**.

Received: June 29, 2011
Published Online: September 12, 2011

